Investigations into the structural, morphology and optoelectronics properties of the CdO:Cu films produced by spray pyrolysis

M. Ahmed[a,*], A. Alshahrie[a,b], E. R. Shaaban[c]
[a]*Department of Physics: Faculty of Science, King Abdulaziz University, 80203, Jeddah, 21589, Saudi Arabia.*
[b]*Center of Nanotechnology, King Abdulaziz University, Jeddah 21589, Saudi Arabia*
[c]*Physics Department: Faculty of Science, Al-Azhar University, P.O. 71452, Assiut, Egypt*

This study used spray pyrolysis to create CdO films that were undoped and doped with Cu at varied concentrations (0, 1, 2, 3, 4 and 5%). The materials' polycrystalline cubic nature is confirmed by XRD examination. Rietveld refinement was used to get the lattice constant. In terms of energy dispersive more about the chemical makeup of materials. The structure, morphological, optical, and electrical properties of the film were investigated using the (XRD), (SEM), UV- spectrophotometer, and Hall arrangement. The band optical gaps, E_g^{opt}, of the CdO:Cu films were observed to decrease as the quantity of Cu doping increased. Also, effective Cu doping enhances the electrical characteristics of CdO, as shown by the film's 3 % resistivity. The carrier concentration is approximately $5x10^{20}$ of that $2.25x10^{20}$ of the undoped film, whereas the amount of Cu doping is approximately ten of that of the CdO film. To increase both optical and electrical properties in a variety of optoelectronic device applications, Cu-CdO films can be used as Transparent Conducting Oxide (TCO) materials.

(Received May 12, 2023; Accepted August 18, 2023)

Keywords: Pyrolysis procedure, CdO:Cu films, Rietveld refinement, Optical energy gap, Electrical parameters

1. Introduction

Transparent conducting oxide materials have recently been the topic of extensive research because of their potential for use in technological products by transmitting visible-range photons and carrying electric charge [1, 2]. Optoelectronics, photovoltaics, photodiodes, and other fields could all benefit greatly from optical transparent conducting oxides with programmable band gaps [3-5]. The n-type semiconductor CdO has an optical gap of 2.5 eV [4]. Owing to its excellent optical transmittance in the visible region and great electrical conductivity, CdO has recently attracted attention as a practical material for solar cell submissions [6]. The CdO-based photodiode displayed that the reverse current of the diode increases by three orders of extent under typical tungsten light [7]. The effect of band gap (nanoparticle size) on the modification performance of the diode was too examined [8]. Doping can also be used to modify CdO's optical characteristics and therefore its band gap [9]. Deokate et al. [10] discovered that F doping increases the optical band gap of pure CdO films. The effects of Sn doping on the optoelectrical properties of CdO film have been well-documented [12]. It was demonstrated that Sn doping causes the optical band gap to shift to the blue and the electrical conductivity to decrease. Dakhel recently released a few studies based on CdO films doped with rare earth elements [13, 14]. According to these publications, light rare earth element doping often causes the optical band gap of CdO films to decrease. Several techniques, such as chemical deposition, spray pyrolysis, chemical vapour deposition, chemical bath deposition, sol-gel, and sputtering, can be used to create both undoped and doped CdO films [15]. The nebulized spray pyrolysis (NSP) method is used in this instance to produce CdO:Cu films since it is straightforward, cost-effective, and able to deposit over vast

* Corresponding author: mhafidh@kau.edu.sa
https://doi.org/10.15251/DJNB.2023.183.1007

areas. This method's ability to create polycrystalline structured films is a key benefit [16]. This work investigates and reports on the structure-morphology, optoelectrical of the Cu-doped CdO film properties.

2. Details of an experiment

2.1. Utilizing the spray pyrolysis coating process, prepare the film

Glass substrates were coated with thin layers using a standard spray pyrolysis coating method. 2.65 grammes of cadmium acetate dehydrate ($Cd(CH_3COO)_22H_2O$) were dissolved in 100 cc of water to create a 0.1 M solution of cadmium acetate. The precursor solution contained dissolved copper chloride ($CuCl_2$.2H2O). The atomic percentage of copper to cadmium was changed from 0 to 1, 2, 3, 4, and 5 at.% to examine the consequence of copper concentration on the physical properties of the CdO films. After a thorough stirring, the solution was heated for roughly 50 minutes at 60 ^oC, until it became bright and ready for spraying. Each sample's substrate temperature was accurately controlled to 300 °C using a temperature controller. The nozzle was 30 cm away from the substrate and the deposition rate was 10 mL/min. The heated plate rotated at a rate of 35 rpm. Glass substrates were prepared for the films by first cleaning them with ethanol in an ultrasonic bath for 20 min. The system was allowed to gradually cool to RT after around 90 minutes. The atomic ratios of copper to tin in the spray solutions used to create the 0-Cu/CdO, 1-Cu/CdO, 2-Cu/CdO, 3-Cu/CdO, 4-Cu/CdO, and 5-Cu/CdO thin films were 0, 1, 2, 3, 4, and 5 (at.%), respectively.

2.2. Materials characterizations

Film samples with 2θ ranging between 5 and 70 have been examined for phase purity and crystal structure using (XRD) Philips diffractometry (1710). EDAX and XR-photoelectron spectroscopy (XPS) were also used to examine the chemical composition of materials. The indicated elements' relative inaccuracy cannot be greater than 2%. To determine the morphologies of the samples, (JEOL-2010) used SEM. The characteristics of the band structure were examined using the XPS method. Using a UV- JASCO-670 spectrophotometer, the absorbance optical spectra of the deposited films were measured at room temperature. Using a quartz cuvette with a thickness of 1 cm, the absorption spectra of materials were captured in the 300–2500 nm range for a dispersed solution (powder dispersed in ethanol). Van der Pauw method and Hall effect experiment were used to measure the electrical properties of 0-Cu/CdO, 1-Cu/CdO, 2-Cu/CdO, 3-Cu/CdO, 4-Cu/CdO, and 5-Cu/CdO films (HMS-5000, ECOPIA). On a glass substrate of 1 cm^2, the resistivity, mobility, and carrier concentration were examined.

3. Results and discussions

3.1. XRD analysis and morphology

Figure 1 shows the XRD patterns of the pure and CdO:Cu thin films (a). The (111), (200), (220), (311), and (311) planes are represented by the five diffraction peaks in this figure, which are situated at angles of 33.01°, 36.03°, 55.27°, 65.71°, and 69.25°, respectively. The peaks support the cubic crystal structure of the pure CdO phase and agree with the baseline JCPDS data (05-0640). The lack of CuO or $Cd(OH)_2$ peaks in the XRD patterns indicates that the host CdO lattice's inclusion of Cu^{2+} ions had no effect on the substance's crystal structure. Because Cu^{2+} ions replace Cd^{2+} ions in the host lattice, the host lattice shrinks (decreased lattice parameter values, Table 1), which results in the (111) peak shifting towards a higher angle with an increase in Cu concentration (Fig. 1 (b)). This is because Cu^{2+} ions have a smaller ionic radius (0.73 nm) than Cd^{2+} ions, which causes the host lattice to contract (0.95 nm). Subsequently, using the Rietveld method, the lattice parameters (a=b=c) of the pure and Cu-doped CdO thin films were determined and refined [18]. In Fig. 1, the results of the Rietveld refinement are shown as an illustration (c). The relatively small discrepancy between the measured and refined intensities, as shown in Fig.

3(c), as well as the lattice parameters and low R-factors listed in Table 1 provide evidence that the refinement was successful.

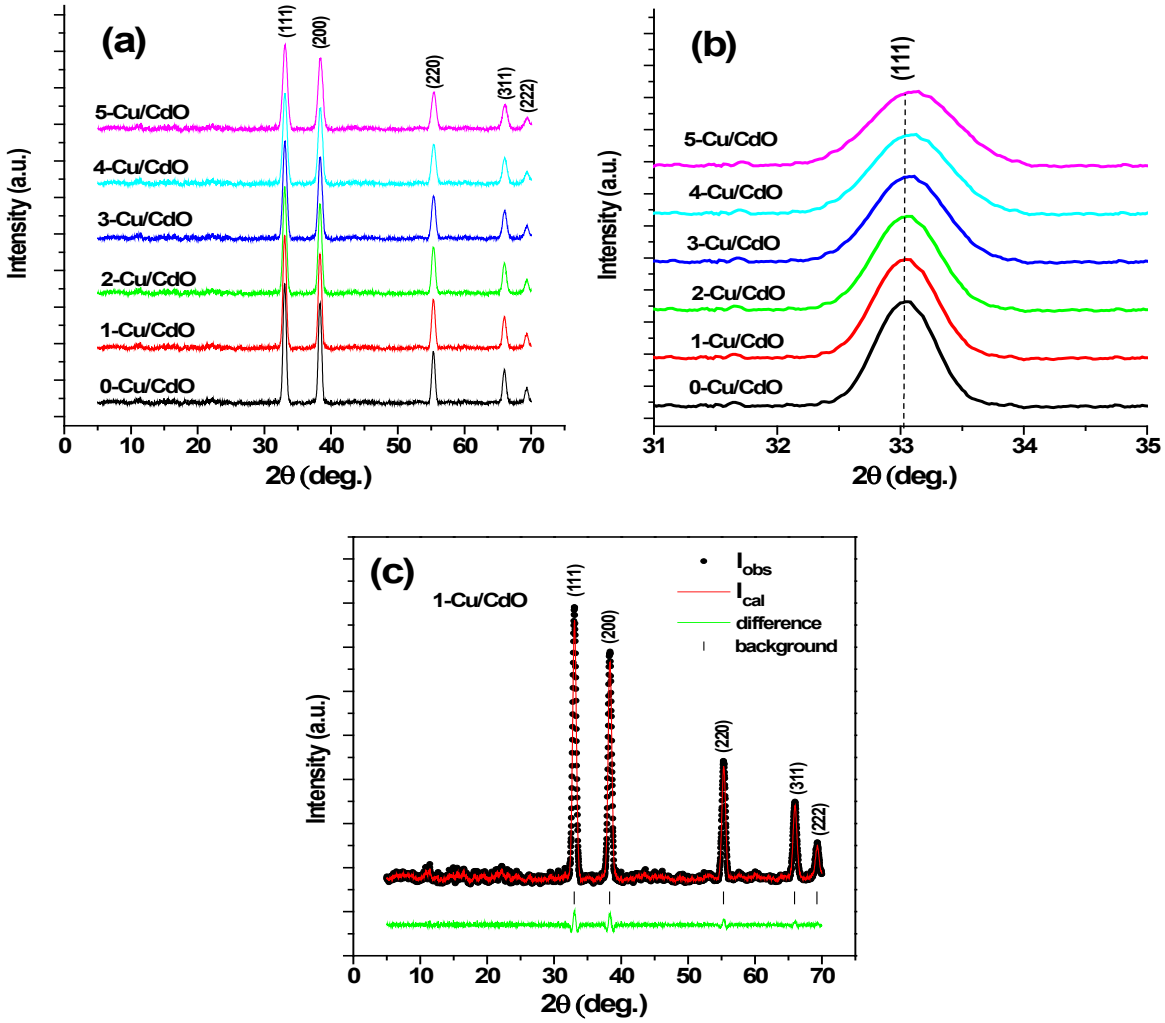

Fig. 1. (a) XRD of CdO:Cu thin films, (b) peak shift of (111) plane and (c) XRD of 1-Cu/CdO film with Rietveld Refinement.

By using the Scherrer ($D = 0.9\lambda / \beta \cos\theta$) and Wilson ($e = \beta / 4\tan\theta$) equations, XRD data were also examined to determine the size of the crystallite, *D*, and macrostrain, *e*, of the CdO:Cu films [17–19]. After correcting ($\beta = \sqrt{\beta_{obs}^2 - \beta_{std}^2}$),

In which β is the broadening equivalent to the variation in profile width between the films, β_{obs}, and the standard (silicon), β_{std}. Figure 2 depicts the reduction in crystallite size brought on by the greater integration of Cu^{2+} ions into the host CdO lattice's Cd^{2+} sites. Also, the variable displacement of the atoms relative to their reference-lattice positions results in lattice strain widening. A reduction in crystallite size and an increase in lattice strain result in the degradation of the crystalline quality of CdO films with Cu doping and an increase in the total grain boundary fraction in the films.

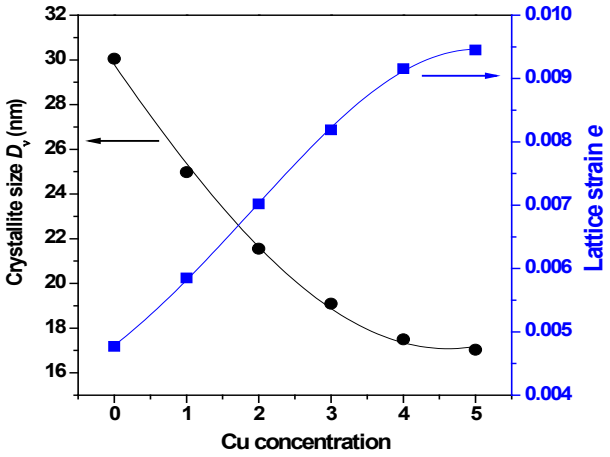

Fig. 2. Average crystallites size and lattice strain versus Cu concentration of $Cd_{1-x}Cu_xO$ films.

Figure 3 illustrates the Energy Dispersive Analysis X-ray (EDAX) profile of two thin films: (a) 1-Cu/CdO and (b) 4-Cu/CdO. The elemental makeup of the generated films was examined using EDAX tests, which also served to validate the successful doping of Cu to CdO films. It's intriguing to note that no extraterrestrial stuff is present in the spectrum. Further evidence of sample purity. All doping samples contained copper peaks and those for cadmium and oxygen, which are given in table 1 by weight percentage. This indicates that doping Cu was successful. This makes it obvious that the strength of Cu grows as the amount of Cu incorporated into CdO increases. Cu was found in the CdO system, and EDAX analysis supported this. The weight percentage was practically the same as the nominal stoichiometry of their films.

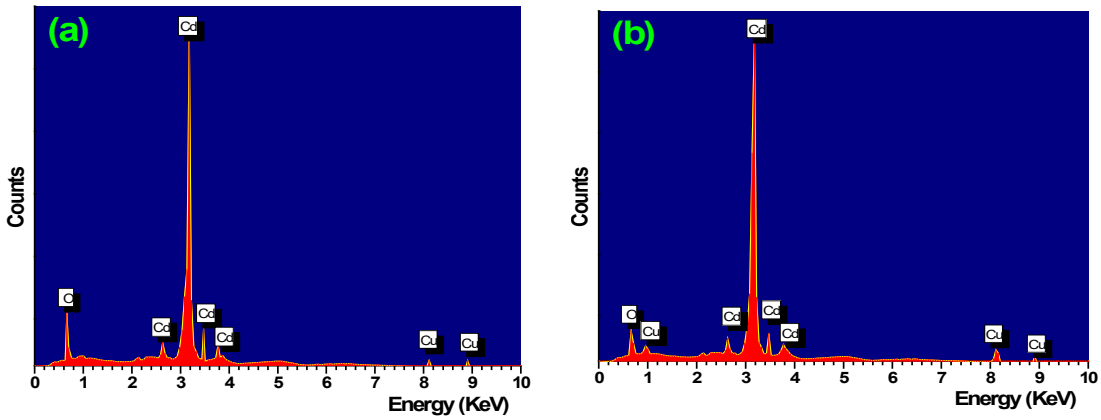

Fig. 3. (a) EDAX of CdO:Cu (a) 1-Cu/CdO and (b) 4-Cu/CdO thin films.

Figure 4 depicts the SEM of thin films with Cu concentrations of 1 weight percent (a) and 4 weight percent (b) correspondingly. It can be seen that the doping of Cu results in a clear reduction in grain size. The average grain size of 1-Cu/CdO and 4-Cu/CdO films is around 37 nm and 26 nm, respectively, with a slightly wider grain size distribution for the former, ranging from 20 nm to 60 nm, and for the latter, from 10 nm to 45 nm. A reduction in average grain size leads to poor crystalline quality and an increase in the overall grain boundary fraction in the films.

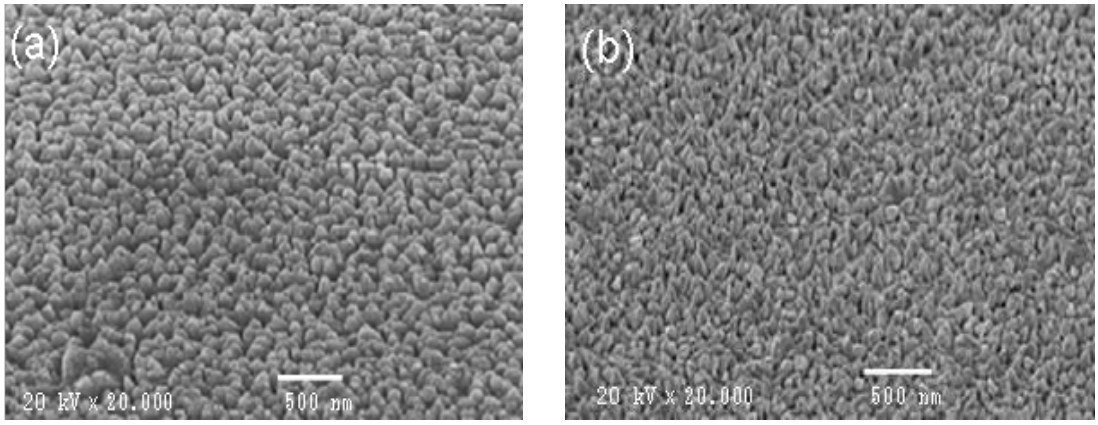

Fig. 4. SEM images for CdO:Cu (a) 1-Cu/CdO and (b) 4-Cu/CdO thin films.

3.2. Optical characterization

Figure 5 reports the absorbance spectra of the CdO:Cu thin films. The derivative of absorbance to wavelength was used to determine the band edge value. Figure 6 displays the derivative of the absorbance of CdO:Cu films as a function of wavelength. The findings of the survey are provided below. The formula E_d^{opt} =hc/λ_{max}, where λ_{max}, is the wavelength of maximum absorption and c is the speed of light, can be used to determine the band edge of thin films from the location of the peak [20, 21]. When the Cu concentration rose, the band edge of the investigated films dropped from 2.55 eV (1-Cu/CdO) films to 2.13 eV (5-Cu/CdO) films. The band gap and optical properties of manufactured Cu doped and bare CdO films are calculated using the Kubelka-Munk function [22] that is αhυ = Á($h\upsilon$- E_g^{opt})^p, where h is the plank constant, υ is the frequency of incident radiation, α is the coefficient of absorption, and p is taken as ½ for direct band gap semiconductors. The band gap values can be obtained by extrapolating the linear section of the figure between hυ and $(\alpha h\upsilon)^2$. When Cu concentration rose, the band edge of the investigated films dropped from 2.51 eV (1-Cu/CdO) films to 2.28 eV (5-Cu/CdO) films. Figure 8 shows the band edge and energy gap values in relation to the Cu content. The structural distortion in the CdO films brought on by the substitution of Cu ions for either interstitial or substitutional Cd ions in the CdO lattice may be the source of the reduction in the optical band gap detected with increased Cu doping. These Cu ions would slightly raise the energy levels of the CdO band gap in the direction of the valence band edge, reducing the energy required for the direct transition [23]. Moreover, the Burstein-Moss effect or the sp-d exchange interactions between the localised d electrons and the band electrons of the Cu^{2+} ions that replace Cd^{2+} ions may be responsibility for the detected red shift in the optical band gap value [24, 25]. Subsequently, Cu doping in CdO films, Saha et al. [26] reported a comparable reduction in the band gap from 2.53 to 2.51 eV. Doping with rare earth elements has also been connected to a similar decline in the band gap of CdO [12, 13, 27]. Despite multiple reports of Cu-doped ZnO films, the literature review finds no evidence of Cu doping in CdO films [28, 29]. Using Cu doping, Wang and Lin [30] saw a drop in the band gap of ZnO films from 3.31 to 3.16 eV. While having a low relative to other conducting oxide thin films, CdO is not a typical TCO material. In most anticipated applications, a varied band gap is theoretically favoured for TCO [31, 32]. Widen E_g^{opt} thus has a lot of practical applications. TCO films, for instance, are used in solar cell applications where more performance is always necessary. As a result, CdO:Cu thin films showed elevated transmission in the higher intensity and energy portion of the solar spectrum, between 500 and 600 nm [33]. So, in addition to their improved electrical properties, CdO:Cu films have likely to be used for optical heaters, photovoltaic solar cells, transparent electrodes, and other optoelectronic devices.

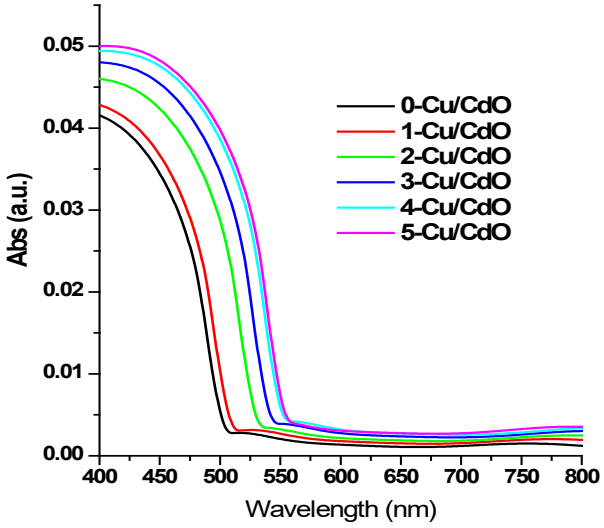

Fig. 5. Absorbance spectra for CdO:Cu thin films.

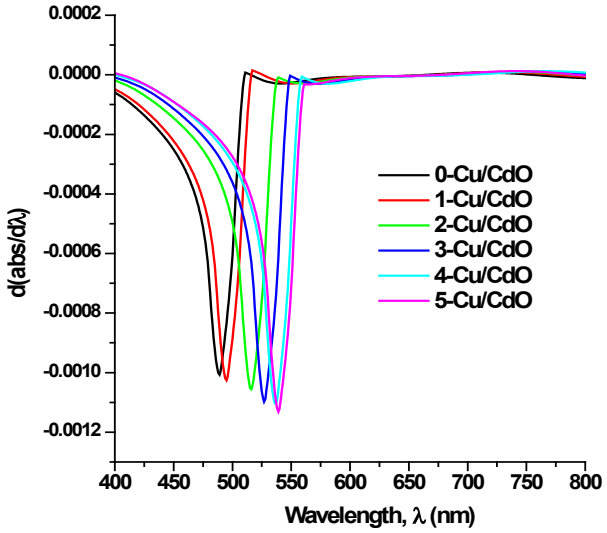

Fig. 6. Spectra of the absorbance derivative CdO:Cu thin films.

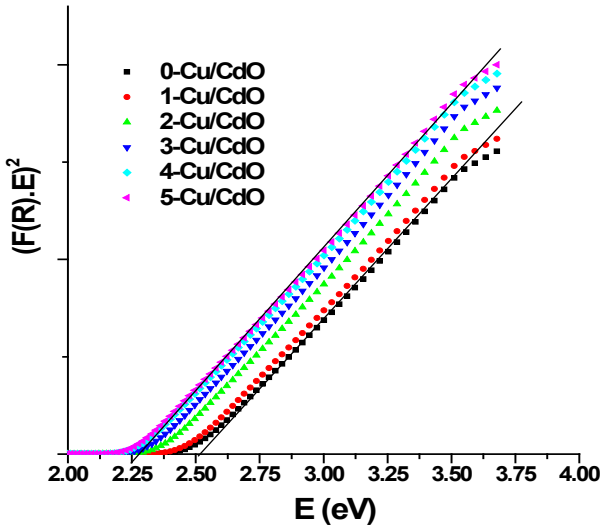

Fig. 7. The dependence of $(\alpha.hv)^2$ on hv for the different compositions of CdO:Cu films.

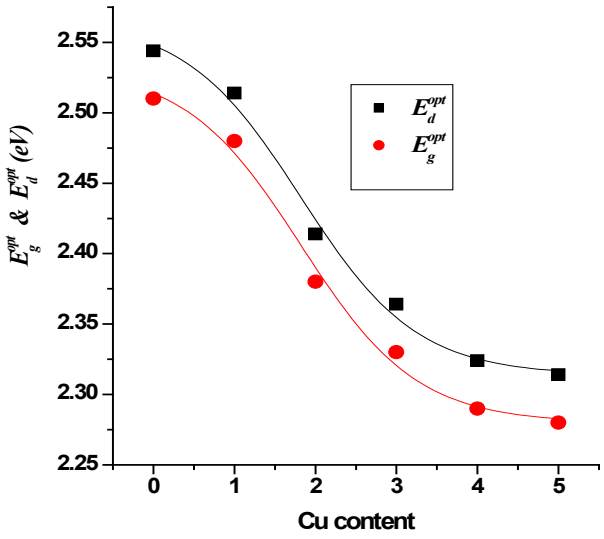

Fig. 8. Band edge and energy gap as a function of Cu content for different compositions of CdO:Cu films.

3.3. Electrical characteristics

The van der Pauw arrangement was used for the Hall measurements, which were conducted at RT. The found negative gradient in the magnetic field against Hall voltage plots provided evidence that the conducting carriers in all samples were n-type. Fig. 9 depicts the differences in electrical characteristics as a function of Cu doping concentration. The resistivity of the produced CdO:Cu thin films reduces when Cu content climbs to 3 at.%, and rises to 4 and 5 weight percent. The carrier concentration of the CdO:Cu thin films, on the other hand, rapidly increases for the film with 3 at% Cu doping and then drops as the Cu doping concentration is raised. The interstitial diffusion of Cu^{2+} ions in the CdO lattice may be the cause of the rise in carrier concentration because they improve the defect state, which can release free electrons into the conduction band and greatly boost carrier concentration. However, as shown in Fig. 9, the carrier mobility of the CdO:Cu film dramatically decreases when Cu doping is increased to 4 and 5 at%. When the solubility limit of Cu in CdO is exceeded, extra Cu atoms may occupy interstitial places because the covalent radius of Cu^{+2} (1.17) is smaller than that of Cd^{2+} (1.48). As a result, the crystal lattice is distorted and grain boundary defects grow, which would impede or scatter carrier transport. As a result, as the amount of Cu-doping rises, the mobility of an undoped CdO film approaches a maximum and subsequently decreases. The induced ionised impurity scattering centres in these films may potentially be responsible for the decrease in mobility at higher dopant concentrations. According to the current experimental findings, the thin film of 3 at% CdO:Cu has a low resistivity of 1.73 x 10-4 cm, which is lower than the undoped CdO film's (12 x 10^{-4} cm). Moreover, the films exhibit high carrier concentration, low electrical resistivity, and acceptable mobility at moderate doping concentrations of 3–4 at% Cu, endowing the CdO:Cu thin films with outstanding electrical properties. It is shown that transparent conducting oxides (TCO) films based on CdO frequently exhibit lower resistivity and higher carrier concentration than TCO materials based on In_2O_3- [34], ZnO- [35], and SnO_2- [36].

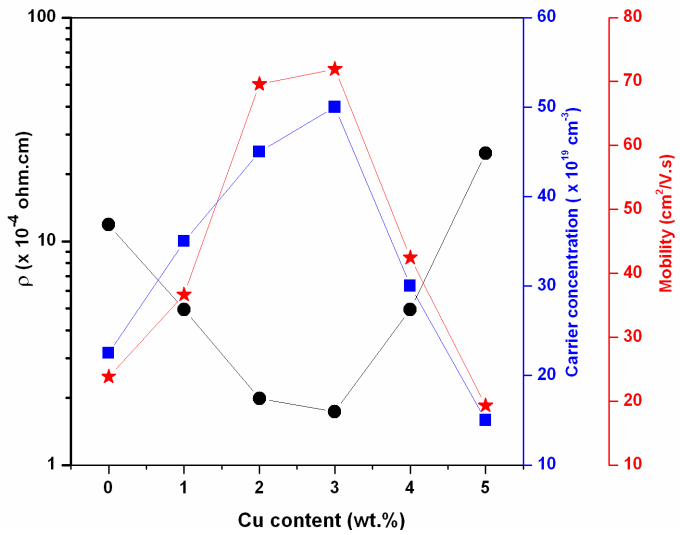

Fig. 9. The resistivityρ, carrier concentrations n Hall mobilityμ, and at RT of CdO:Cu film with various Cu incorporation.

4. Conclusions

Using the use of spray pyrolysis, undoped and Cu:CdO: films are successfully deposited on a glass surface. The structural study reveals a cubic structure that is polycrystalline with highly (111) peak at 33º. When Cu^{2+} ions were occupying the interstitial site in CdO, the peak intensity dropped as a result of Cu incorporation. Change in lattice constant may be caused by the dopant ion (Cu) having a smaller ionic radius than the host ions (Cd). EDAX study of the morphology demonstrates the existence of the Cd, O, and Cu components with stoichiometric composition.

According to optical assessments, the absorbance in the UV region is greater than that in the visible range, and the rise in absorbance with doping concentration may be caused by the transition of electrons from the valence band to the conduction band. With increasing Cu content, the band edge of the examined films fell from 2.51 eV (1-Cu/CdO) to 2.28 eV (5-Cu/CdO) films. Electrical trials revealed that for 4 and 5% Cu-doped films, the resistivity and carrier mobility decreased and rose by up to 3%, respectively. Also, proper Cu doping enhances the electrical characteristics of CdO, as evidenced by the fact that the carrier concentration of a CdO film with 3 % Cu doping is about 5 x 10^{20} times higher than that 2.25 x 10^{20} of an undoped CdO film, while the resistivity is nearly ten times higher. To increase optical and electrical properties in several optoelectronic device applications, CdO:Cu thin films have potential utility as TCO materials.

Acknowledgements

This research work was funded by Institutional Fund Projects under grant no. (IFPIP:1981-130-1443). The authors gratefully acknowledge the technical and financial support provided by the Ministry of Education and King Abdulaziz, DSR, Jeddah, Saudi Arabia

References

[1] Z. Qiao, C. Agashe, D. Mergel, Thin solid films, 496 (2006) 520-525; https://doi.org/10.1016/j.tsf.2005.08.282

[2] S. Jäger, B. Szyszka, J. Szczyrbowski, G. Bräuer, Surface and coatings technology, 98 (1998) 1304-1314; https://doi.org/10.1016/S0257-8972(97)00145-X

[3] R.K. Gupta, K. Ghosh, R. Patel, P.K. Kahol, Mater. Sci. Eng. B 156 (2009) 1; https://doi.org/10.1016/j.mseb.2008.09.051

[4] M. Ravikumar, R. Chandramohan, K.D.A. Kumar, S. Valanarasu, A.Kathalingam, V. Ganesh, M. Shkir, S. AlFaify, H. Algarni, J. Phys. Chem. Solids 118 (2018) 211-220; https://doi.org/10.1016/j.jpcs.2018.03.009

[5] E. Monroy, F. Omnès, F. Calle, Semicond. Sci. Technol. 18 (4) (2003) R33; https://doi.org/10.1088/0268-1242/18/4/201

[6] M Emam-Ismail, M El-Hagary, ER Shaaban, S Althoyaib, Journal of alloys and compounds 529 (2012)113-121; https://doi.org/10.1016/j.jallcom.2012.03.027

[7] Z.A. Alahmed, H.A. Albrithen, A.A. Al-Ghamdi, F. Yakuphanoglu, Optik 126 (5) (2015) 575-577; https://doi.org/10.1016/j.ijleo.2015.01.005

[8] B. Coskun, T. Asar, U. Akgul, K. Yildiz, Y. Atici, Ferroelectrics 502 (1) (2016) 147-158; https://doi.org/10.1080/00150193.2016.1235453

[9] D. Carballeda-Galicia, R. Castanedo-Perez, O. Jimenez-Sandoval, S. Jimenez-Sandoval, G. Torres-Delgado, C. Zuniga-Romero, Thin Solid Films 371 (1) (2000) 105-108; https://doi.org/10.1016/S0040-6090(00)00987-1

[10] E. R. Shaaban, M. S. Abd El-Sadek, M. El-Hagary, I. S. Yahia, Physica Scripta 86 (1), (2012) 015702; https://doi.org/10.1088/0031-8949/86/01/015702

[11] A.A. Dakhel, J. Mater. Sci. 46 (2011) 1455; https://doi.org/10.1007/s10853-010-4946-x

[12] ER Shaaban, M El-Hagary, M Emam-Ismail, MB El-Den, Philosophical Magazine 91 (12) (2011)1679-1692; https://doi.org/10.1080/14786435.2010.544683

[13] A.A. Dakhel, J. Alloys Compd. 475 (2009) 51; https://doi.org/10.1016/j.jallcom.2008.08.008

[14] A.A. Dakhel, Mater. Chem. Phys. 117 (2009) 284-7; https://doi.org/10.1016/j.matchemphys.2009.06.003

[15] E. R. Shaaban, M. Mohamed, M. N. Abd-el Salam, A.Y. Abdel-Latief, M. A. Abdel-Rahim, Optical Materials 86 (2018) 318-325;https://doi.org/10.1016/j.optmat.2018.10.027

[16] A.S. Riad, S.A. Mahmoud, A.A. Ibrahim, Physica B Condens. Matter 296 (4) (2001) 319-325; https://doi.org/10.1016/S0921-4526(00)00571-8

[17] A.L. Patterson, Phys. Rev. 56 (1939) 978-982; https://doi.org/10.1103/PhysRev.56.978

[18] A Goel, ER Shaaban, MJ Ribeiro, FCL Melo, JMF Ferreira, Journal of Physics: Condensed Matter 19 (38) (2007) 386231; https://doi.org/10.1088/0953-8984/19/38/386231

[19] D Prakash, AM Aboraia, M El-Hagary, ER Shaaban, KD Verma, Ceramics International 42 (2) (2016) 2676-2685; https://doi.org/10.1016/j.ceramint.2015.10.096

[20] El-Hagary, M., Shaaban, E.R., Moustafa, S.H., Gad, G.M.A. Solid State Science 2019, 91, 15-22; https://doi.org/10.1016/j.solidstatesciences.2019.03.005

[21] ER Shaaban, M El-Hagary, M Emam-Ismail, MB El-Den, Philosophical Magazine 91 (12) (2011) 1679-1692; https://doi.org/10.1080/14786435.2010.544683

[22] P. Kubelka, and F. Z. Munk, Tech. Phys. 12 (1931) 5.

[23] Kim, P.Y., Lee, J.Y., Lee, H.Y., Lee, S.J. and Cho, N.I. (2008), Journal of Korean Physical Society, 53, 207-211; https://doi.org/10.3938/jkps.53.207

[24] E. Burstein, Phys Rev; 93 (1954) 632; https://doi.org/10.1103/PhysRev.93.632

[25] T. S. Moss TS. Proc Phys Soc London B 1954;67 (1954) 775; https://doi.org/10.1088/0370-1301/67/10/306

[26] M. Alzaid, A Qasem, E. R. Shaaban, N. M. A. Hadia, Optical Materials 110 (2020)110539; https://doi.org/10.1016/j.optmat.2020.110539

[27] A.A. Dakhel, Sol. Energy 83 (2009) 934; https://doi.org/10.1016/j.solener.2008.12.015

[28] K. Chandra Sekhar Reddy, P. Sahatiya, I. Santos-Sauceda, O. Cortázar, R.Ramírez-Bon, Appl.Surf. Sci. 513 (2020), 145804; https://doi.org/10.1016/j.apsusc.2020.145804

[29] Cristina Maria Vladut, Mihaiu 1 Susana, Tenea 1 Ecaterina, Silviu Preda, JoseM. Calderon-Moreno, Anastasescu 1 Mihai, Hermine Stroescu, Irina Atkinson,Mariuca Gartner, Carmen Moldovan, Maria Zaharescu, J. Nanomater. (2019); https://doi.org/10.1155/2019/6269145

[30] R.C. Wang, H.Y. Lin, Mater. Chem. Phys. 125 (2011) 263; https://doi.org/10.1016/j.matchemphys.2010.09.021

[28] K. Chandra Sekhar Reddy, P. Sahatiya, I. Santos-Sauceda, O. Cortázar, R.Ramírez-Bon, Appl.Surf. Sci. 513 (2020), 145804; https://doi.org/10.1016/j.apsusc.2020.145804

[31] M. Ravikumar, R. Chandramohan, K.D.A. Kumar, S. Valanarasu, A.Kathalingam, V. Ganesh, M. Shkir, S. AlFaify, H. Algarni, J. Phys. Chem. Solids 118 (2018) 211-220; https://doi.org/10.1016/j.jpcs.2018.03.009

[32] AA Dakhel, Bulletin of Materials Science 43 (1) (2020)13; https://doi.org/10.1007/s12034-020-02104-8

[33] C. A. Gueymard, Solar Energy 2008;82 (2008) 260; https://doi.org/10.1016/j.solener.2007.04.007

[34] S. Parthiban, E. Elangovan, K. Ramamurthi, R. Martins, and E. Fortunato: Sol. Energy Mater. Sol. Cells 94 (3) (2010) 406; https://doi.org/10.1016/j.solmat.2009.10.017

[35] Y. D. Liu and J. S. Lian, Applied Surface Science, vol. 253, no. 7, (2007) 3727-3730; https://doi.org/10.1016/j.apsusc.2006.08.012

[36] S Nakao, N Yamada, T Hitosugi, Y Hirose, T Shimada, T Hasegawa, Thin Solid Films 518 (2010) 3093; https://doi.org/10.1016/j.tsf.2009.09.187